An investigation of the role of recombination processes in the operation of InAs/GaAs$_{1-x}$Sb$_x$ quantum dot solar cells

Y. Cheng[1], A. J. Meleco[1], A. J. Roeth[1], V. R. Whiteside[1], M. C. Debnath[1], M. B. Santos[1], T. D. Mishima[1], S. Hatch[2], H-Y. Liu[2], and I. R. Sellers[1]

[1]Homer L. Dodge Department of Physics & Astronomy, University of Oklahoma, Norman, OK

[2]Department of Electrical & Electronic Engineering, University College London, Torrington Place. London. WC1E 7JE. U. K

***Abstract* — The electroluminescence and photoluminescence from an InAs/GaAs$_{1-x}$Sb$_x$ quantum dot solar cell are investigated as a function of temperature and correlated to the PV characteristics of the cell over the same temperature range. Analysis of the dominant recombination mechanism is shown to change from radiative to non-radiative above ~ 150 K, which is consistent with a *reduction* in the J_{sc} (and V_{oc}) at evaluated temperatures in these devices.**

I. Introduction

Single band gap solar cells are limited to efficiencies on the order of 30% as described by the Shockley-Queisser limit [1]. Intermediate band solar cells (IBSC) [2] have been proposed as a candidate system to overcome this limit through the absorption of sub-gap photons with a potential efficiency of greater than 60 % under ideal conditions [2][3] . The creation of an intermediate band (IB) requires the formation of an isolated band within the band gap of the absorber material. The 3-dimensional confinement of semiconductor quantum dots (QDs) makes them a candidate system to form such IBs. Several QD systems have been studied in the past decade [4]-[9]; InAs/GaAs QDs being the most well investigated material system for IBSC applications [4]-[6][9][11]. However, by replacing the GaAs matrix material with GaAs$_{1-x}$Sb$_x$, a higher density of QDs has been demonstrated [12][13] with a better spectral match to the solar resource [14].

II. Experiment Details

The InAs/GaAs$_{1-x}$Sb$_x$ QD solar cell studied in this work was grown by molecular beam epitaxy (MBE). The InAs/GaAs$_{1-x}$Sb$_x$ QD structure, which serves as the intrinsic region, is repeated 5 times and sandwiched within p- and n-type GaAs layers to form a p-i-n diode architecture. The composition of the the GaAs$_{1-x}$Sb$_x$ matrix was x = 0.14 to achieve a *quasi*-flat valence band (VB) as determined for this system previously [12][13].

III. Results and Discussions

Figure 1(a) compares the photoluminescence (*PL*) and electroluminescence (*EL*) for the QD region at various temperatures. The *EL* displays a single peak at 1050 nm (77 K), 1130 nm (210 K), and 1153 nm (298 K), respectively. The *PL* at 77 K and 210 K display much broader emission consistent with non-idealities and bimodality in the system; which are presumably quenched or saturated at the higher injection levels present in *EL*.

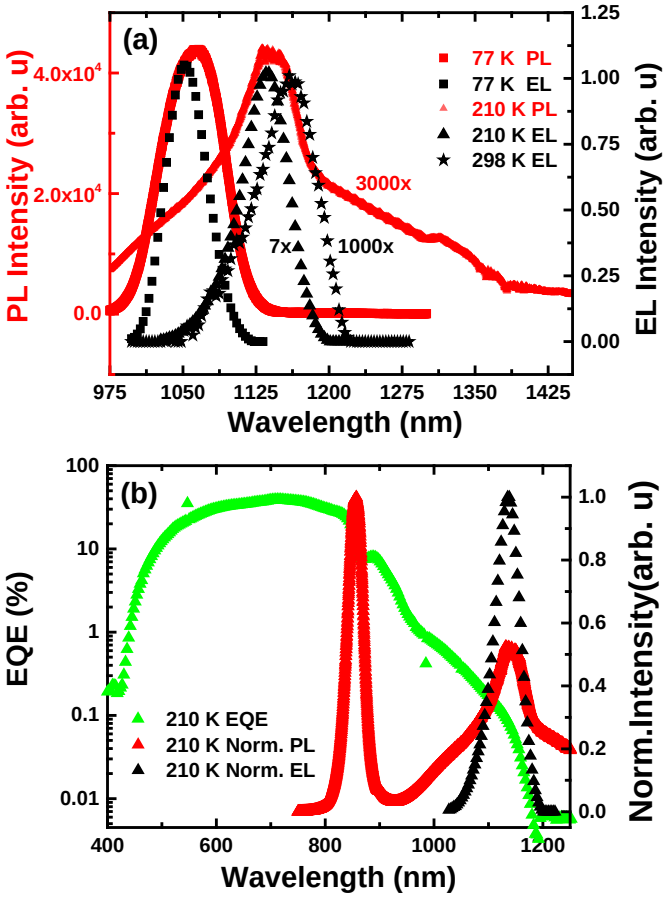

Figure 1 (a) *PL* (red symbols) and *EL* (black symbols) spectra at 77 K (squares), 210 K (triangles), and *EL* at room temperature (stars); (b) Normalized *PL* (red triangles), *EL* (black triangles), and *EQE* (green triangles) at 210 K.

Figure 1(b) shows a comparison of the external quantum efficiency (*EQE*) of the device at 210 K to illustrate that the single peak evident in the *EL* measurements is indeed related to the QD transition; i.e., the VB to IB transition in the active

region of the device. Figure 1(b) also shows the normalized *PL* measured at 210 K, which displays two additional features not evident in the *EL*: at 870 nm and 970 nm - correlating to absorption in the GaAs and GaAsSb matrix, respectively. The absence of these features in the *EL* measurements reflects the direct injection of the carriers into the QDs and the separation of the quasi-fermi level that is set by the difference in energy of the QD transitions in *EL*. In the PL measurements the GaAs emitter and QDs are probed simultaneously [15] which, with the combination of the longer radiative lifetime of photogenerated carriers in the type-II QDs, contributes to significant *PL* from the continuum regions.

By T = 210 K, the *PL* shows a three order of magnitude reduction in intensity and is similar in strength to a broad (900 – 1500 nm) defect band; which dominates the *PL* as the temperature is increased above 210 K (not shown here). This defect band reflects the contribution of dislocations in the matrix region that result during growth due to the significant lattice mismatch (1.4 %) between GaAs and GaAsSb regions [12] [16]. At low temperatures, photogenerated carriers (electrons) in the QDs are isolated from these defect centers due to the strong confinement of the QDs. However, at elevated temperatures the increased thermal energy not only facilitates the photogenerated carriers to transfer between QDs but also, the defect states now serve as efficient single particle non-radiative recombination centers for these mobile carriers - dominating the *PL* spectra. The rapid loss of the photogenerated carriers indicates the absence of a well isolated intermediate band in the system. Indeed, evidence of carrier extraction at 77 K (not shown, see [12]) indicates the absence of such an IB at all temperatures measured (above 77 K) in the current series of samples.

The PL recombination processes at low and high temperature have been presented previously and appear to indicate two regimes: (1) a low temperature regime, in which photogenerated carriers are isolated and recombine directly in the QDs.; (2) a higher temperature (> 160 K) region within which carriers have enough thermal energy to escape from the QDs where they experience considerable non-radiative loss due to exposure to defects and traps. These non-radiative recombination process serve to simultaneously increase the reverse saturation (dark) current in current-voltage (*J-V)* measurements and reduce the open circuit voltage.

The non-radiative recombination of the QDs is also observed to be correlated to a reduction in the *EL* intensity *except* this reduction occurs at slightly higher temperatures than that of the *PL* (above 210 K). This may be explained by a partial saturation of defects in the matrix at increasing injection levels during *EL*. Previous measurements of temperature dependent *J-V* and *EQE* [12] also indicated a transition in which carrier recombination significantly affects the performance of the device with large reductions in open circuit voltage (V_{oc}) with increasing temperature. At T < 160 K, the radiative recombination of the carriers served as the limiting effect in the extraction of the photogenerated carriers; while non-radiative recombination, facilitated by thermally activated non-radiative centers, was deemed responsible for poor carrier extraction and large increase (decrease) in the dark current (V_{oc}) at higher temperature (T > 210 K).

These two regimes displayed very unconventional (non-monotonic) photocurrent behavior whereby, a slightly increasing short circuit current density (J_{sc}) was observed between 77 K and 160 K reaching a minimum point at 170 K; above 170 K, the J_{sc} fluctuated (see Figure 2 (b)). This complex behavior is attributed to a transition from the dominance of radiative to non-radiative processes at elevated temperatures, along with the competing processes of carrier extraction (increasing $\boldsymbol{J_{sc}}$) and recombination (decreasing $\boldsymbol{J_{sc}}$).

To further investigate these hypotheses, here, we present a comparison of the spontaneous emission in *EL* measurements to determine the nature and dominance of the recombination processes under different conditions and correlate these findings to the PV analysis. The current injected into a device can be approximated by [17]:

$$I = eV(An + Bn^2 + Cn^3) + I_{leak} \ . \qquad (1)$$

Where *A*, *B*, and *C* represent: single carrier (defect-mediated) recombination, radiative recombination, and Auger-mediated process coefficients, respectively [17]. *V and e* are the active region volume and electronic charge, respectively.

Single carrier recombination is associated with the recombination through traps and defects (Shockley-Reed-Hall) [17]; the radiative recombination is related to the *spontaneous emission (EL).* The total integrated spontaneous emission rate L is proportional to the radiative recombination n^2. Equation (1) can be further simplified to $I \propto n^z \propto L^{1/2^z}$ such as to allow a correlation between current injection (*I*), spontaneous emission (*L*), and the dominant recombination mechanism (*n*) [17] to be determined. When radiative recombination dominates the current, the *z*-factor will be close to 2 ($\propto n^2$). However, if *z* is closer to 1 ($\propto n$), this indicates the current is dominated by non-radiative recombination centers - defects and traps.

By plotting $\ln(I) - \ln(L^{1/2})$, *z* can be extracted from the slope to determine the nature of the recombination processes. Figure 2 (a) shows data along with a linear fit for 4 different temperatures from 77 K to 298 K. The slope becomes shallower as the temperature increases, which indicates a reduction of *z*. The temperature dependent behavior of *z* is shown in Figure 2 (b). Between T = 77 K and T = 150 K, the *z*-factor remains above 2. This indicates that the current is dominated (predominately) by radiative recombination, with some contribution from Auger-processes, at higher injection. Losses due to defect-mediated non-radiative processes, however, appear limited below T = 150 K.

As the temperature is increased above 150 K, *z* decreases towards ~1 at room temperature, indicating the increasing dominance of non-radiative processes at elevated temperatures. The decrease of *z* corresponds directly to the temperature dependent (TD) reduction in *EL* intensity (or radiative efficiency). This is qualitatively consistent to that evident in the TD *PL* and steady decrease in V_{oc} evident in the

TD *J-V* under 1-sun illumination [12] [16]. These results serve to further reflect the thermally activated behavior of the non-radiative changes as a function of temperatures.

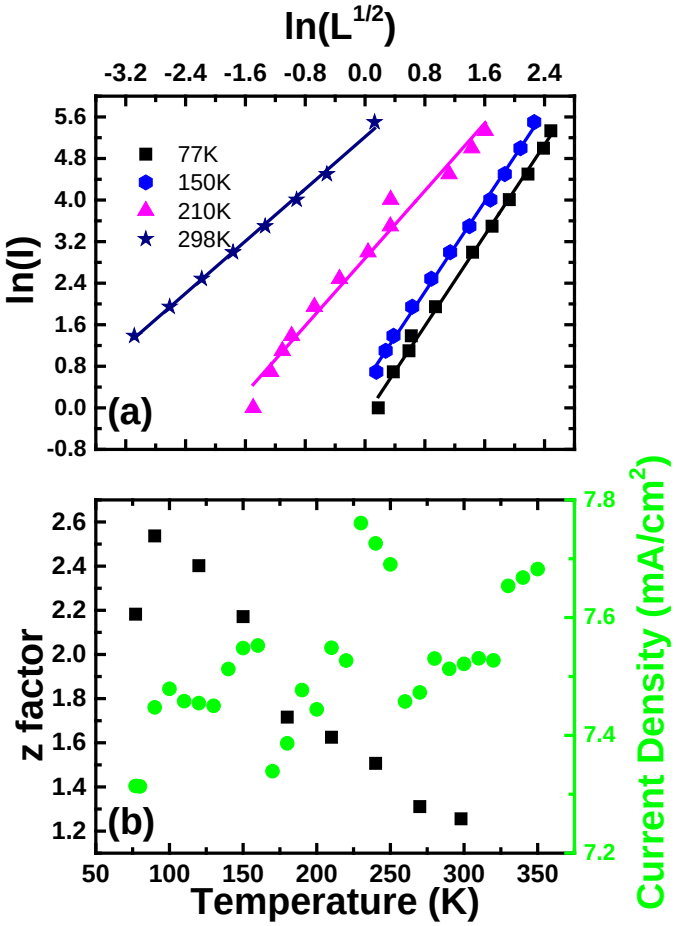

Figure 2 (a) ln (I)- ln($L^{1/2}$) at 77 K, 150 K, 210 K and 298 K; (b) Temperature dependent behavior of Z-factor (black squares) , Jsc extracted from the J-V measurements (green circles).

IV. Conclusion

An InAs/$GaAs_{0.86}Sb_{0.14}$ QDSC was investigated using complementary *PL* and *EL* measurements to support previous measurements on a series of similar structures that show unusual escape and transport mechanisms. A rapid quenching of the *PL* and *EL* intensity, along with a transition (above 150 K) in the dominant recombination process (*z*-factor) in high temperature *EL* measurements further indicate the prevalence of non-radiative processes at elevated temperatures in these systems. This correlates qualitatively with TD *EQE* and *J-V* measurements - supporting the conclusion that non-radiative processes introduced by the lattice mismatch between the GaAsSb matrix and GaAs perturbs the transport behavior of the QDs; suggesting further improvements in material growth and quality are required before these systems can be considered practical for applications in IBSCs.

V. Acknowledgment

Supported is acknowledged through the Oklahoma Center for the Advancement of Science & Technology (ONAP 09-08, AR09.2-019, and OARS AR12.2-043).

References

[1] W. Shockley and H. J. Queisser, "Detailed balance limit of efficiency of p‐n junction solar cells." *Journal of applied physics* 32.3 (1961): 510-519.

[2] A. Luque, and A. Martí. "Increasing the efficiency of ideal solar cells by photon induced transitions at intermediate levels." *Physical Review Letters* 78.26 (1997): 5014.

[3] A. Luque and A. Martí, "The intermediate band solar cell: progress toward the realization of an attractive concept." *Advanced Materials* 22, no. 2 (2010): 160-174.

[4] S. M. Hubbard, C. D. Cress, C. G. Bailey, R. P. Raffaelle, S. G. Bailey, and D. M. Wilt, "Effect of strain compensation on quantum dot enhanced GaAs solar cells." *Applied Physics Letters* 92, no. 12 (2008): 123512.

[5] G. Jolley, H. F. Lu, L. Fu, H. H. Tan, and C. Jagadish, "Electron-hole recombination properties of $In_{0.5}Ga_{0.5}$ As/GaAs quantum dot solar cells and the influence on the open circuit voltage." *Applied Physics Letters* 97, no. 12 (2010): 123505.

[6] K. A. Sablon, J. W. Little, K. A. Olver, Z. M. Wang, V. G. Dorogan, Y. I. Mazur, G. J. Salamo, and F. J. Towner, "Effects of AlGaAs energy barriers on InAs/GaAs quantum dot solar cells." *Journal of Applied Physics* 108, no. 7 (2010): 074305.

[7] P. J. Simmonds, R. B. Laghumavarapu, M. Sun, A. Lin, C. J. Reyner, B. Liang, and D. L. Huffaker, "Structural and optical properties of InAs/AlAsSb quantum dots with GaAs (Sb) cladding layers." *Applied Physics Letters* 100, no. 24 (2012): 243108.

[8] R. B. Laghumavarapu, A. Moscho, A. Khoshakhlagh, M. El-Emawy, L. F. Lester, and D. L. Huffaker, "GaSb⁄ GaAs type II quantum dot solar cells for enhanced infrared spectral response." *Applied Physics Letters* 90, no. 17 (2007): 173125.

[9] S. Hatch, J. Wu, K. Sablon, P. Lam, M. Tang, Q. Jiang, and H. Liu, "InAs/GaAsSb quantum dot solar cells." *Optics express* 22, no. 103 (2014): A679-A685.

[10] F. K. Tutu, I. R. Sellers, M. G. Peinado, C. E. Pastore, S. M. Willis, A. R. Watt, T. Wang, and H. Y. Liu, "Improved performance of multilayer InAs/GaAs quantum-dot solar cells using a high-growth-temperature GaAs spacer layer." *Journal of Applied Physics* 111, no. 4 (2012): 046101.

[11] A Martí, E. Antolín, C. R. Stanley, C. D. Farmer, N. López, P. Díaz, E. Cánovas, P. G. Linares, and A. Luque. "Production of photocurrent due to intermediate-to-conduction-band transitions: a demonstration of a key operating principle of the intermediate-band solar cell." *Physical Review Letters* 97, no. 24 (2006): 247701.

[12] Y. Cheng, M. Fukuda, V. Whiteside, M. Debnath, P. Vallely, T. Mishima, M. Santos, K. Hossain, S. Hatch, H. Liu, et al., M. Fukuda, V. R. Whiteside, M. C. Debnath, P. J. Vallely, T. D. Mishima, M. B. Santos et al. "Investigation of InAs/$GaAs_{1-x}Sb_x$ quantum dots for applications in intermediate band solar cells." *Solar Energy Materials and Solar Cells* 147 (2016): 94-100.

[13] Debnath, M. C., T. D. Mishima, M. B. Santos, Y. Cheng, V. R. Whiteside, I. R. Sellers, K. Hossain, R. B. Laghumavarapu, B. L. Liang, and D. L. Huffaker. "High-density InAs/GaAs1− x Sb x quantum-dot structures grown by molecular beam epitaxy for use in intermediate band solar cells." *Journal of Applied Physics* 119, no. 11 (2016): 114301.
[14] M. Y. Levy and C. Honsberg, "Nanostructured absorbers for multiple transition solar cells." *IEEE Transactions on Electron Devices* 55, no. 3 (2008): 706-711.
[15] I. Ramiro, E. Antolín, P. G. Linares, E. Hernández, A. Martí, A. Luque, C. Farmer, and C. Stanley. "Application of photoluminescence and electroluminescence techniques to the characterization of intermediate band solar cells." *Energy Procedia* 10 (2011): 117-121.
[16] Y. Cheng, M. Fukuda, V. R. Whiteside, M. C. Debnath, P. J. Vallely, A. J. Meleco, A. J. Roeth et al. "Investigation of InAs/GaAs$_{1-x}$Sb$_x$ quantum dots for applications in intermediate band solar cells." *Photovoltaic Specialists Conference (PVSC)*, 2016 IEEE 43rd, pp. 0005-0008, 2016
[17] A. F. Phillips, S. J. Sweeney, A. R. Adams, and P. J. Thijs. "The temperature dependence of 1.3-and 1.5-um compressively strained InGaAs (P) MQW semiconductor lasers." *IEEE Journal of selected topics in quantum electronics* 5, no. 3 (1999): 401-412.